The University Of Sheffield.

This is a repository copy of *Thermal analysis and control development of interior PM traction machines*.

White Rose Research Online URL for this paper:
http://eprints.whiterose.ac.uk/150222/

Version: Accepted Version

Proceedings Paper:

Hoang, K.D. orcid.org/0000-0001-7463-9681, Atallah, K., Lazari, P. et al. (2 more authors) (2019) Thermal analysis and control development of interior PM traction machines. In: Proceedings of IECON 2019 - 45th Annual Conference of the IEEE Industrial Electronics Society. IECON 2019 : 45th Annual Conference of the IEEE Industrial Electronics Society (IES), 14-17 Oct 2019, Lisbon, Portugal. IEEE , pp. 1399-1404. ISBN 9781728148793

https://doi.org/10.1109/IECON.2019.8927023

© 2019 IEEE. Personal use of this material is permitted. Permission from IEEE must be obtained for all other users, including reprinting/ republishing this material for advertising or promotional purposes, creating new collective works for resale or redistribution to servers or lists, or reuse of any copyrighted components of this work in other works. Reproduced in accordance with the publisher's self-archiving policy.

Reuse

Items deposited in White Rose Research Online are protected by copyright, with all rights reserved unless indicated otherwise. They may be downloaded and/or printed for private study, or other acts as permitted by national copyright laws. The publisher or other rights holders may allow further reproduction and re-use of the full text version. This is indicated by the licence information on the White Rose Research Online record for the item.

Takedown

If you consider content in White Rose Research Online to be in breach of UK law, please notify us by emailing eprints@whiterose.ac.uk including the URL of the record and the reason for the withdrawal request.

White Rose university consortium
Universities of Leeds, Sheffield & York

eprints@whiterose.ac.uk
https://eprints.whiterose.ac.uk/

Thermal Analysis and Control Development of Interior PM Traction Machines

Khoa Dang Hoang, Kais Atallah, and Panagiotis Lazari
Dept. of Electronic and Electrical Engineering
The University of Sheffield
Sheffield, United Kingdom
https://orcid.org/0000-0001-7463-9681
https://orcid.org/0000-0002-8008-8457
p.lazari@sheffield.ac.uk

Jeff Birchall and Stuart Calverley
Magnomatics Limited
Park House, Bernard Road
Sheffield, S2 5BG, United Kingdom
j.birchall@magnomatics.com
s.calverley@magnomatics.com

***Abstract*—The paper presents thermal analysis and control development for interior permanent magnet (IPM) traction machine. Losses of the IPM traction machine are discussed and derived using measurement and finite element analysis. The loss components are then employed for steady-state and transient thermal analysis. Assuming rotor temperature obtained from transient thermal simulation over driving cycles, *dq*-axis current reference LUTs employing on the traction machine drive system are determined. It is shown that when steady state rotor temperature is higher than the average driving cycle temperature, maximum difference in electromagnetic torque is less than 5.5% over the torque-speed envelope.**

Keywords*—Copper loss, cooling system, IPM traction machine, iron loss, thermal analysis.

I. Introduction

Due to its abilities on high-torque and widen-speed range performance [1], [2], interior permanent magnet (IPM) machines are often selected for traction applications where short-period overload and deep field-weakening (FW) operations associated with high machine temperature is normally required. In practice, unexpected high temperature in IPM machine may result in reducing on machine lifetime, degrading of machine insulation, and partly or fully demagnetizing of its PM rotor [3]. Thus, thermal analysis for determination of a relevant cooling system is an essential step during earlier stage of design and control development for traction machine. For IPM machine to be operated in deep FW region, high eddy-harmonic iron loss significantly contributing on machine high temperature is inevitable [4]. As a result, temperature analysis of the IPM traction machine under its full operated torque-speed range should be considered for cooling system determination. The main focus of this paper is on the continuous rated torque condition.

On the other hand, in control development for IPM traction machine, *dq*-axis current reference look-up tables (LUTs) predefined with a given PM rotor temperature is often employed [1]. However, it is noted that traction applications often do not have a settled steady state operation of which a fixed PM rotor temperature can be defined. Thus, transient temperature profiles over different driving cycles are essential to define PM rotor temperature for *dq*-axis current reference LUTs.

In the paper, a thermal analysis on design and control development of IPM traction machine is introduced. First, losses of IPM traction machine are discussed and analyzed. Then, thermal profile of the tested IPM traction machine following its torque-speed range is evaluated. It is shown that for the tested machine with conventional water-jacket cooling system, the total rotor losses (only around 5% to 10% of its entire stator losses) may result in an extreme high temperature on the rotor side leading to a risk of demagnetizing PM rotor. Thus, a combined cooling solution including water jacket and rotor oil spray is selected for the tested IPM traction machine. Transient thermal analysis associated with the utilized cooling system over different driving cycles is then employed to define rotor temperature for *dq*-axis current reference LUTs implemented on the traction machine drive system.

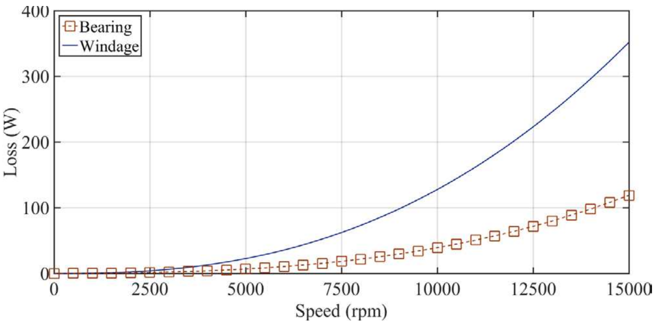

Fig. 1. Windage and bearing losses of tested machine.

TABLE I

SPECIFICATIONS OF TESTED IPM MACHINE

Peak torque (Nm)	225
Continuous torque (Nm)	112.5
Peak current (A)	340
Base speed (rpm)	4850
Maximum speed (rpm)	14600
DC-link voltage (V)	600
Number of pole pair	4

II. Mechanical Losses of IPM Machine

In practice, mechanical losses of the tested machine, Table I, are mainly contributed by windage loss and bearing loss associating with temperature in the rotor side [5].

A. Windage Losses

According to [5], [6], windage loss of rotating rotor P_{wd} including rotor surface air windage loss (P_{ar}) and rotor end-plate disk windage loss (P_{ad}) can be expressed as shown in (1) to (3)

$$P_{wd} = P_{ar} + P_{ad} \tag{1}$$

$$P_{ar} = \pi k_{fr} \rho_a \omega_m^3 l_{stk} D_{or}^4 / 16 \tag{2}$$

$$P_{ad} = k_{fd} \rho_a \omega_m^3 (D_{or}^5 - D_{ir}^5) / 64 \tag{3}$$

where k_{fr} and k_{fd} is the friction coefficient factors of rotor surface and rotor end-plate disk; ρ_a is the air density depending on operating temperature; ω_m is the rotor mechanical speed; l_{stk} is the rotor stack length; D_{ir} is the rotor inner diameter; D_{or} is the rotor outer diameter.

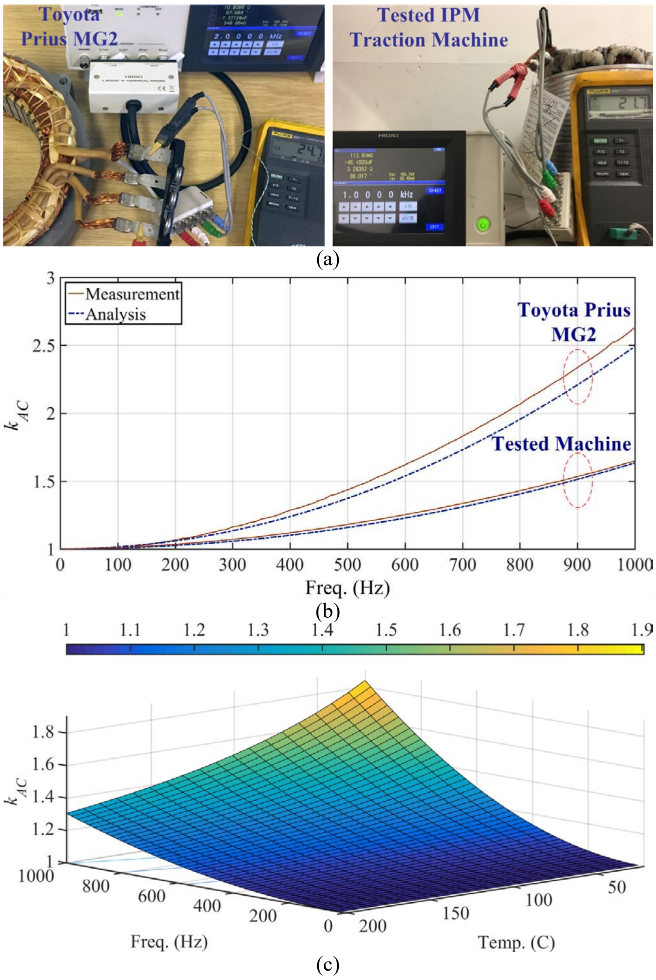

Fig. 2. AC loss analysis. (a) Measurement setup. (b) Measured results. (c) AC loss factor of tested IPM traction machine.

Fig. 1(b) presents windage loss estimated using (1) to (3) for the tested machine up to its maximum operated speed (14600rpm).

B. Bearing Losses

Using the maximum speed (14600rpm) and maximum achievable torque related to the rotor shaft diameter, SKF bearing 6007 is selected for the tested machine and its mechanical loss over torque-speed envelope obtained from the manufacturer [7] is presented in Fig. 1(b). It is noted that the bearing loss depends on different factors such as operating temperature, lubrication, and contamination… [5], [7].

III. Electromagnetic Losses of IPM Machine

A. Copper Losses Considering Temperature Variation and AC Loss

For IMP traction machine operated with short-period overload and deep FW operation, stator winding copper losses are highly affected by temperature variation and high fundamental frequency (AC loss) [5]. In (4) to (6), stator resistance as a function of temperature and fundamental frequency $R_{s(T,f)}$ is presented [8] where $R_{s(T0)}$ is the stator resistance at 20 Celsius degree; ΔT is the delta temperature; r_{tc} is the copper resistivity coefficient; $\rho_{Cu(T0)}$ is the copper resistivity at 20 Celsius degree; $k_{AC(T,f)}$ is the AC loss factor (ratio between DC and AC resistance) as a function of temperature and fundamental frequency; s_{dpt} is the stator slot depth; s_{dm} is the winding strand diameter; $\delta_{(T,f)}$ is the skin-depth as a function of temperature and fundamental frequency; and μ_{Cop} is the copper relative permeability.

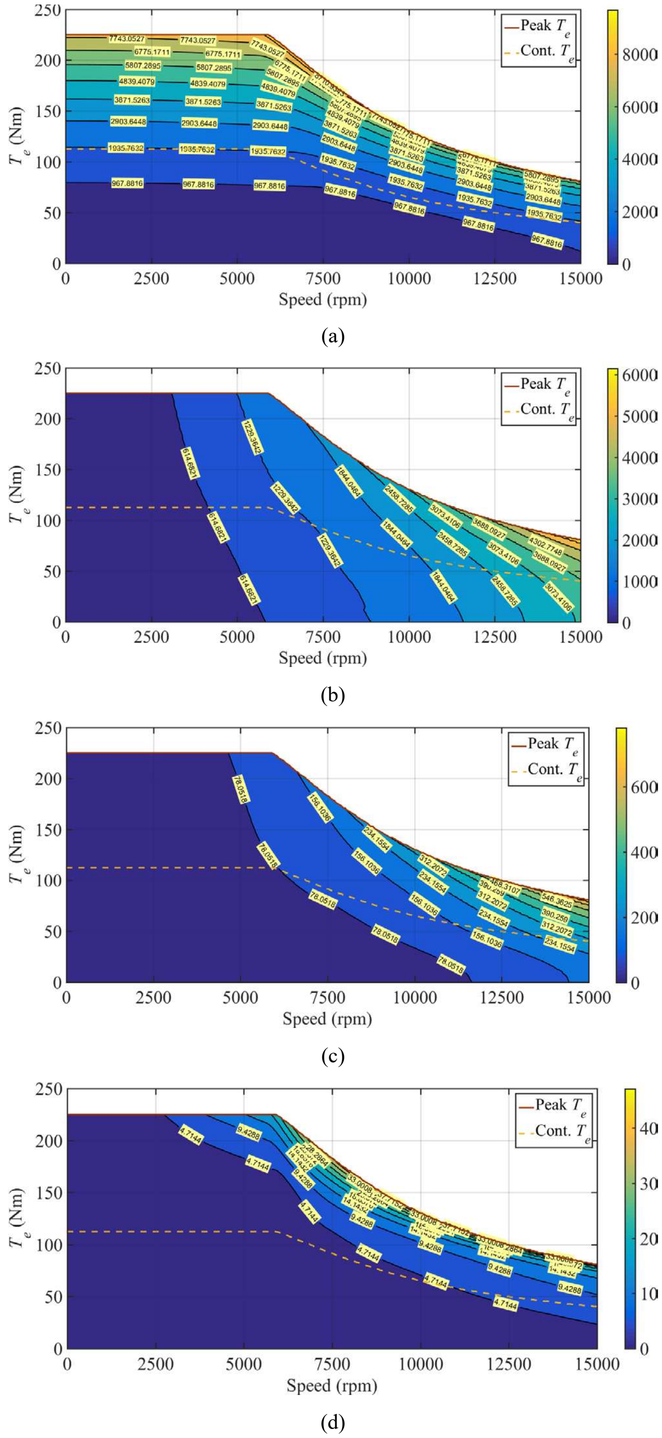

Fig. 3. Electromagnetic losses of tested IPM traction machine. (a) Copper loss. (b) Stator iron loss. (c) Rotor iron loss. (d) PM loss.

Table II

Thermal Material Limitation of Tested IPM Machine

Material	Maximum Temp.	Limitation Temp.
Copper	220	150
PM	220	120
Magnetic steel	NA	NA

$$R_{s(T,f)} = (1 + r_{tc}\Delta T / \rho_{Cu(T0)}) R_{s(T0)} k_{AC(T,f)} \tag{4}$$

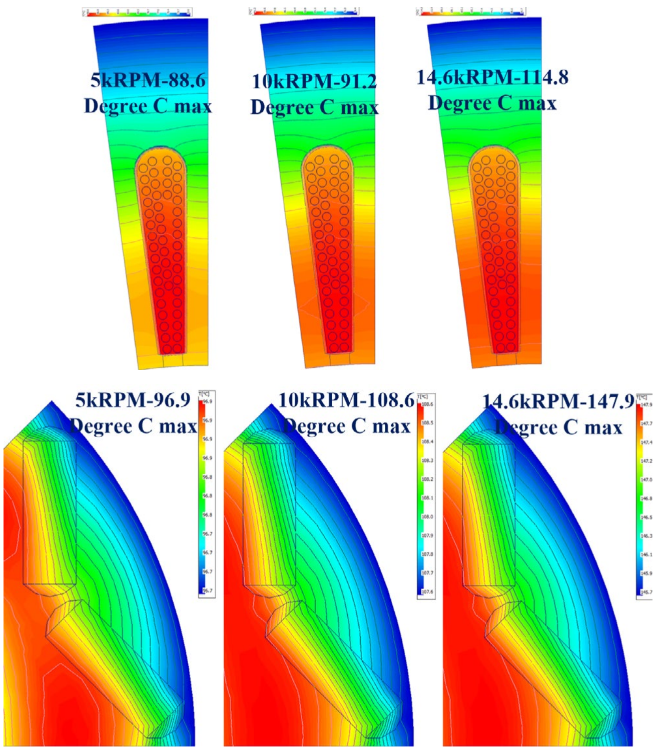

(a)

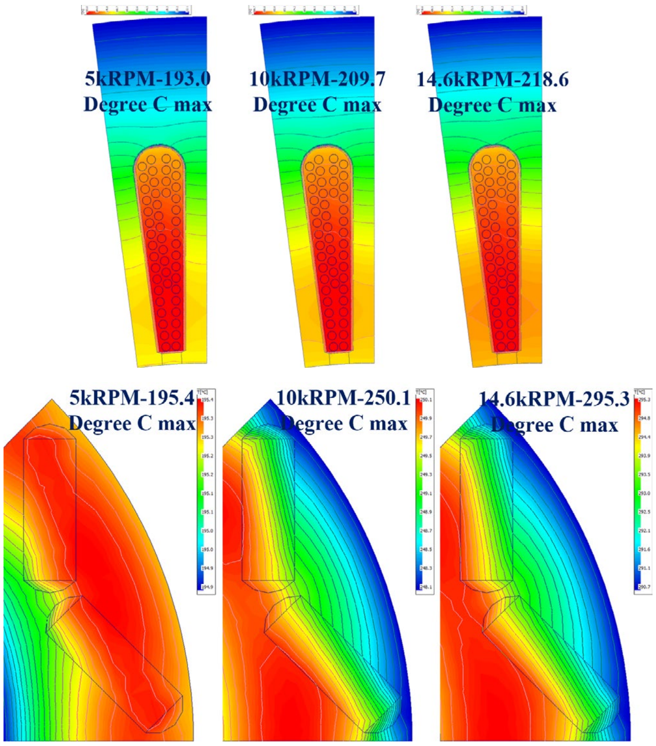

(b)

Fig. 4. Steady-state thermal analysis of tested IPM machine with WJ cooling system. (a) Continuous rated torque. (b) Peak torque.

$$k_{AC(T,f)} = 1 + (1/9)(s_{dpt} / \delta_{(T,f)})^2 (s_{dm} / \delta_{(T,f)})^2 \tag{5}$$

$$\delta_{(T,f)} = \sqrt{(2\rho_{Cop(T)}) / (2\pi f \mu_{Cop})} \tag{6}$$

The AC loss factor in (5) is validated via measurement, Fig. 2(b), using impedance analysis for a traction machine (Toyota Prius MG2) and the tested machine, Fig. 2(a). Based on (5), AC loss factor of the tested machine as a function of operated fundamental frequency and copper temperature is computed and illustrated in Fig. 2(c). Copper loss at 150 Celsius degrees (average rating winding temperature) of the tested machine for a full torque-speed range considering AC loss is depicted in Fig. 3(a).

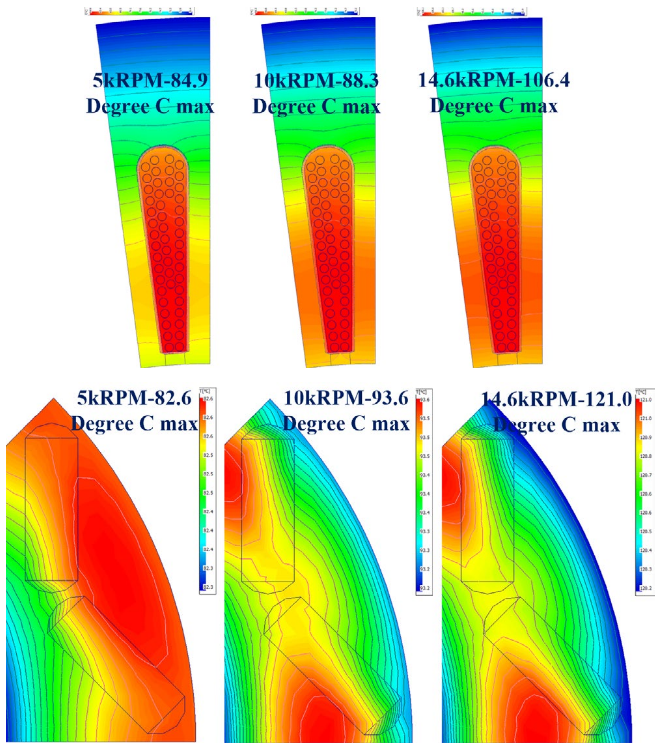

(a)

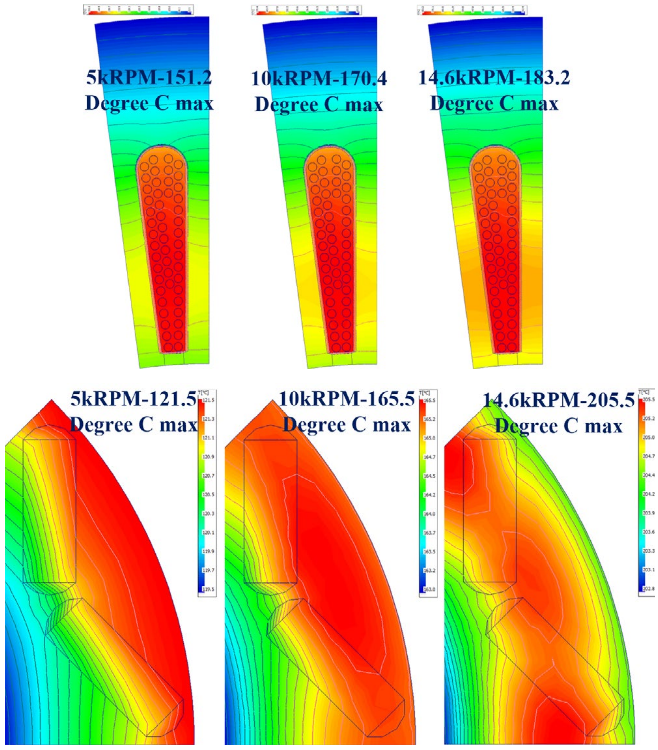

(b)

Fig. 5. Steady-state thermal analysis of tested IPM machine with WJ and ROS cooling system. (a) Continuous rated torque. (b) Peak torque.

B. *Iron Losses*

IPM traction machine iron losses including stator iron loss, rotor iron loss, and PM loss [5], [9] are shown in Figs. 3(b) to 3(d). It is noted that for the tested IPM traction machine, total rotor electromagnetic losses (rotor iron loss and PM loss) is around 5% to 10% of the entire stator electromagnetic losses (stator iron loss and copper loss) over full torque-speed operation.

IV. Thermal Analysis of IPM Machine and Cooling System Determination

A. Material Thermal Limitations

The tested IPM traction machine is designed and developed for integration into a hybrid powertrain of which a water jacket (WJ) cooling system with a flowrate as 6 liter per minute and an inlet coolant temperature as 60 Celsius degree is employed. The stator copper winding is designed with class H of which insulation rating up to 220 Celsius degree and average winding temperature rating around 150 Celsius degree can be achieved. In terms of PM material, high temperature resistant PM (N42-EH) is selected. It is noted that in practice, a thermal limitation up to 120 Celsius degree should be maintained for rotor PM to avoid partly demagnetizing. It is also noted that due to its high Curie temperature (around 700 Celsius degree), thermal limitation consideration of the employed magnetic steel (M270-35A) is unnecessary. The maximum and limitation temperature of the tested machine materials are presented in Table II.

B. Steady-State Thermal Analysis with Water Jacket Cooling System

Based on loss components over continuous/peak torque-speed operation in section II and III, steady-state thermal analysis simulation for the tested machine with water jacket cooling system and ambient temperature as 60 Celsius degree is presented in Fig. 4. As can be seen, higher temperature than the limitation values, Table II, for both stator copper and rotor PM can be observed when the tested machine is operated with continuous rated torque demands in the deep FW region, Fig. 4(a), or peak torque demands over torque-speed envelope, Fig. 4(b). Thus, the employed WJ cooling system may not be adequate enough.

C. Steady-State Thermal Analysis with Water Jacket and Rotor Oil Spray Cooling System

In Fig. 4, higher temperature in rotor side than stator copper winding can be noticed. Thus, a rotor oil spray (ROS) solution with a flowrate as 1 liter per minute and inlet temperature as 90 Celsius degree is considered together with stator casing water jacket (WJ) to maintain temperature of the tested machine within its limited values. Fig. 5 presents steady-state temperature obtained from thermal analysis simulation for the tested machine. As can be seen, the combined cooling solution may manage the machine temperature around its limited values in Table II excepting when it is operated at deep FW region with peak torque demand, Fig. 5(b). However, in practice, these operated conditions are rarely required for the tested machine and it also takes a long period of time for the rotor temperature to reach to this steady state value (further discussion will be presented in the next section).

Based on thermal analysis simulation, a combined cooling solution including stator casing WJ and ROS is developed for the tested machine. Fig. 6 shows the stator casing equipped with water jacket and rotor with inlet pipe for oil spraying. For sensing stator winding temperature, three thermistors (PT1000) with temperature range from -50 to 600 Celsius degree is installed within the stator side. On the other hand, rotor temperature information is extracted from machine back-EMF measurement.

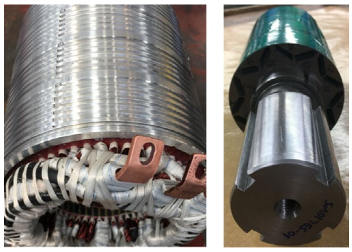

(a)

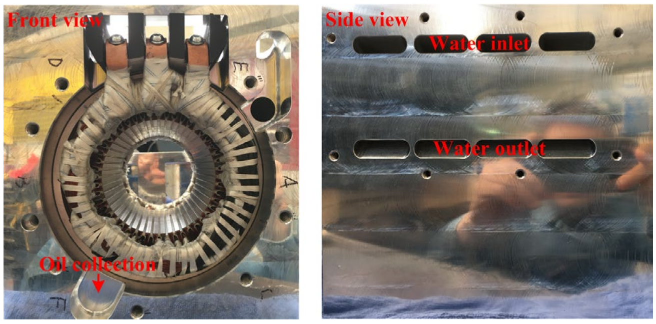

(b)

Fig. 6. Selected cooling system for tested IPM traction machine. (a) Stator with WJ and rotor with ROS. (b) Closed view of cooling system.

V. Control Development for Tested IPM Machine Considering Transient Thermal Analysis

A. Transient Thermal Analysis of Tested IPM Machine over Different Driving Cycles

As aforementioned, the tested IPM traction machine is designed and developed for integration into a hybrid powertrain. Fig. 7 shows its loss components and thermal analysis simulation with the selected cooling system over different driving cycles. As can be seen, temperature of the tested machine using the cooling system with combined solution is maintained lower than 80 Celsius degrees over studied driving cycles which satisfies the thermal material limitations in Table II. It is noted that it takes a long period of time for the rotor temperature to be increased from the ambient temperature to its maximum value.

B. Control Development Using Transient Thermal Analysis

As shown in Fig. 7, rotor temperature of the tested IPM traction machine may not be exceed 80 Celsius degree during its transient operation within the integrated hybrid powertrain. Therefore, a *dq*-axis current reference LUTs based on a fixed rotor PM temperature as 80 Celsius degree is generated for control development of the tested IPM traction machine, Fig. 8.

However, as aforementioned, the rotor temperature value may increase higher that 80 Celsius degree under steady-state operation condition, Fig. 5(a). Therefore, a comparative study in terms of current references for different rotor temperature is illustrated in Fig. 9 where it is shown that an increase of rotor temperature may require the variation of both *dq*-axis currents to maintain a constant torque demand. Fig. 10 presents the torque difference associated with rotor temperature variation. A maximum 5.5% torque difference may be expected when rotor temperature is increased up to

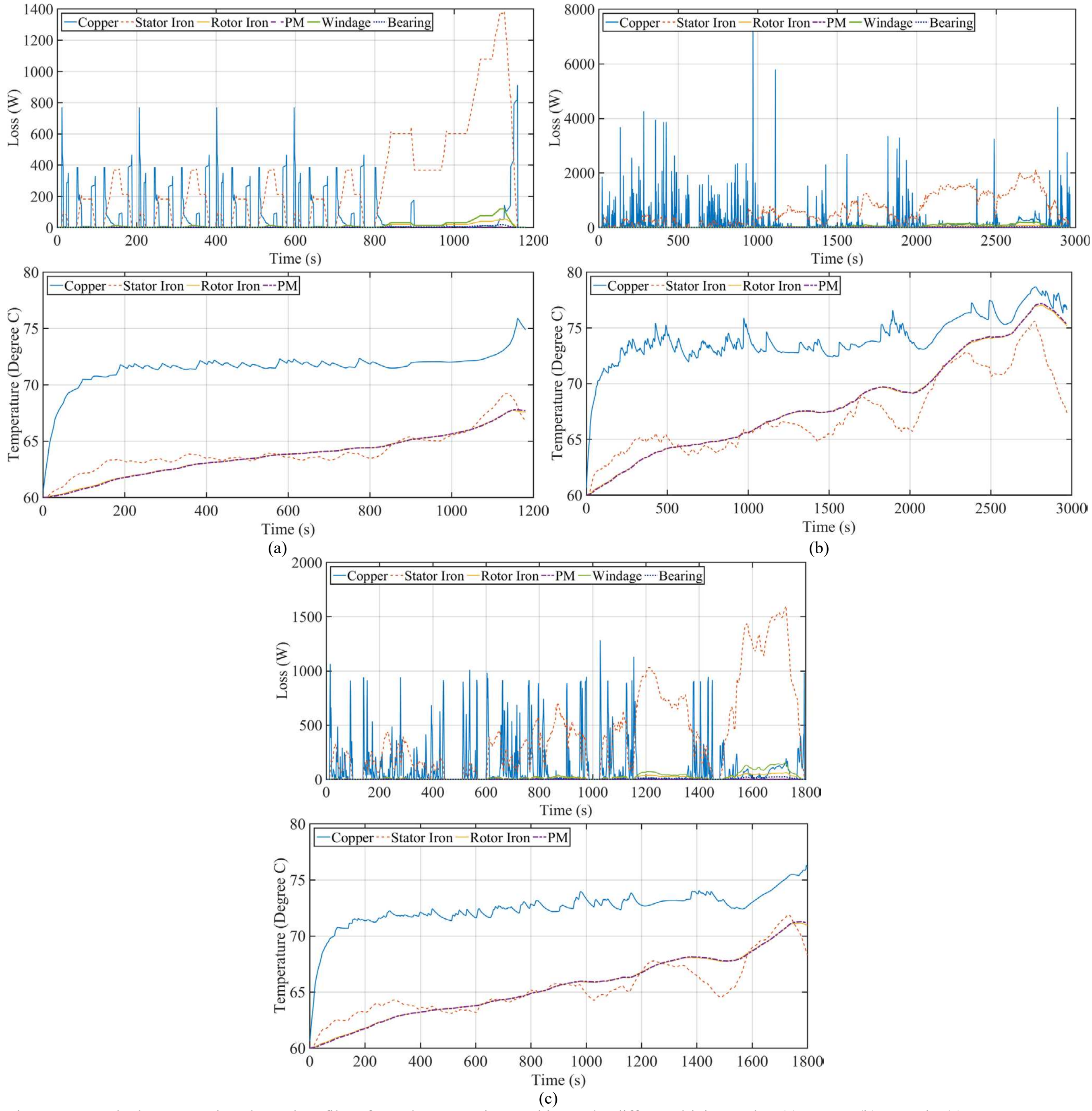

Fig. 7. Loss and relevant transient thermal profiles of tested IPM traction machine under different driving cycles. (a) NEDC. (b) Artemis. (c) WLTP.

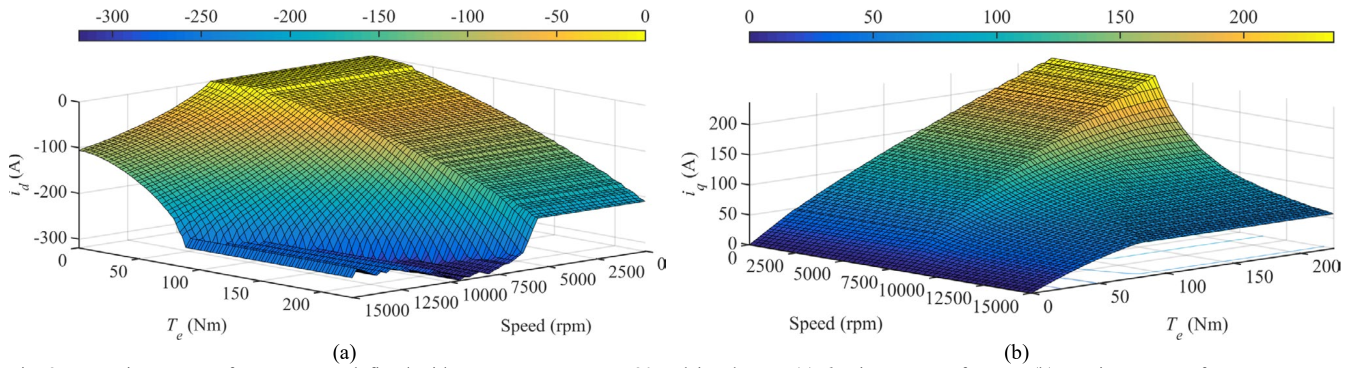

Fig. 8. Dq-axis current reference LUTs defined with rotor temperature as 80 Celsius degree. (a) *d*-axis current reference. (b) *q*-axis current reference.

its maintained limitation value as 120 Celsius degree, Fig. 10(a). In an unexpected extreme case with rotor temperature to be increased up to 150 Celsius degree, a maximum 13% torque difference be forecasted, Fig. 10(b).

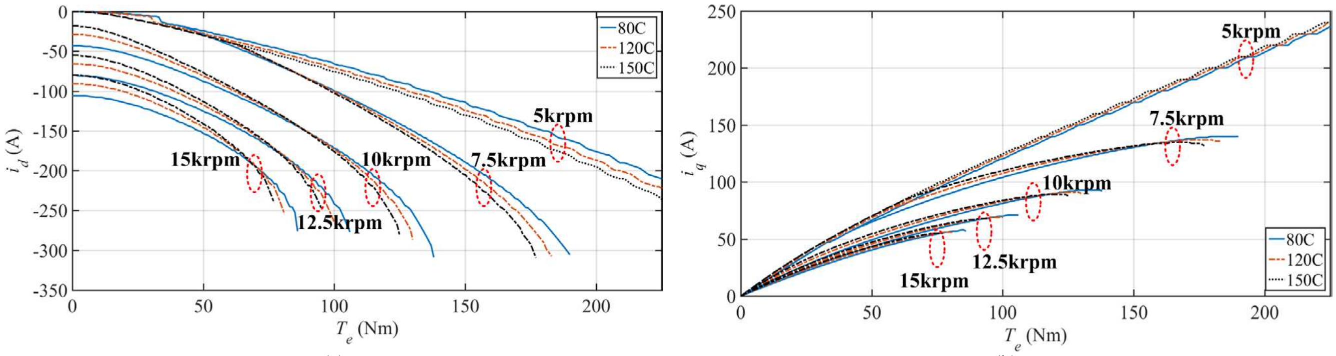

(a) (b)

Fig. 9. Current references of tested IPM traction machine under different rotor temperatures. (a) *d*-aixs current reference. (b) *q*-axis current reference.

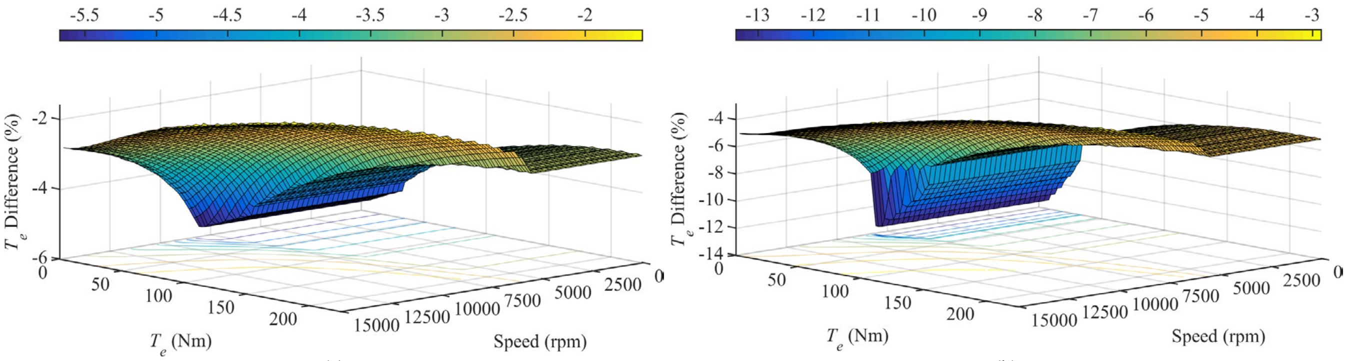

(a) (b)

Fig. 10. Torque differences when rotor temperature is increased higher than 80 Celsius degree. (a) Up to 120 Celsius dergee. (b) Up to 150 Celsius degree.

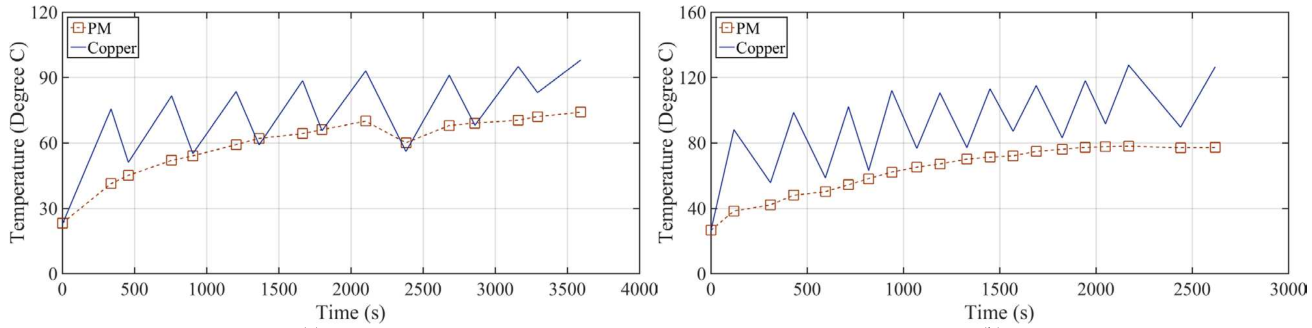

(a) (b)

Fig. 11. Temperature measurement of winding copper and PM at 2000rpm and different intermittent overload torque demands. (a) 150Nm. (b) 200Nm.

Measurement of the temperature rise for the tested IPM machine with selected cooling system under different intermittent overload torque demands (150Nm for up to 1 hour and 200Nm for up to 45 minutes) is presented in Fig. 11. As can be seen, although under overload torque demand, both temperature rises in stator winding copper and rotor PM are maintained lower than their limitation, Table II.

VI. Conclusions

In the paper, thermal analysis and control development for IPM traction machine designed for integrating into a hybrid powertrain has been presented. Taking into consideration of mechanical and electromagnetic losses over the operating torque-speed envelope, appropriate cooling system has been designed and transient thermal simulation over driving cycles are obtained. The average rotor temperature over driving cycles are then used to determine the *dq*-axis current reference LUTs employing in the drive system. Measurement on the test-rig was presented to demonstrate the selected cooling methodology.

References

[1] K. D. Hoang, J. Wang, M. Cyriacks, A. Melkonyan and K. Kriegel, "Feed-forward torque control of interior permanent magnet brushless AC drive for traction applications," *in Proc. IEEE Int. Conf. Electric Mach. Drives (IEMDC) 2013*, Chicago, IL, US, pp. 152-159, 2013.

[2] K. D. Hoang and K. Atallah, "A rapid sizing concept of interior permanent magnet machine for traction applications," *in Proc. IET Int. Conf. Power Electron. Mach. Drives (PEMD)* 2018, Liverpool, United Kingdom, Apr. 17-19, 2018.

[3] J. R. Wang and G. C. Heyns, "Thermal analysis of a water-cooled interior permanent magnet traction machine," *2013 IEEE International Conference on Industrial Technology (ICIT)*, Cape Town, 2013, pp. 416-421.

[4] V. Zivotic-Kukolj, W. L. Soong, and N. Ertugrul, "Iron loss reduction in an interior PM automotive alternator," *IEEE Trans. Ind. Appl.*, vol. 42, no. 6, pp. 1478-1486, Nov./Dec. 2006.

[5] J. F. Gieras, "Permanent magnet motor technology: Design and application," CRC Press, 2010.

[6] E. Vrancik, "Prediction of windage power loss in alternators," NTRS-NASA, Oct. 1968.

[7] https://www.skf.com/uk/products/bearings-units-housings/index.html

[8] D. C. Hanselman and W. H. Peake, "Eddy-current effects in slot-bound conductors," in *IEE Proceedings - Electric Power Applications*, vol. 142, no. 2, pp. 131-136, March 1995.

[9] https://www.motor-design.com/publications/tutorials/

[10] https://www.arnoldmagnetics.com/wp-content /uploads /2017 /11/ N42EH-151021.pdf.